Eur. Phys. J. A **23**, 223–234 (2005)
DOI 10.1140/epja/i2004-10087-7

THE EUROPEAN PHYSICAL JOURNAL A

Two-neutrino double-β decay of $94 \leq A \leq 110$ nuclei for the $0^+ \rightarrow 0^+$ transition

R. Chandra[1], J. Singh[1], P.K. Rath[1], P.K. Raina[2,a], and J.G. Hirsch[3]

[1] Department of Physics, University of Lucknow, Lucknow-226007, India
[2] Department of Physics, IIT Kharagpur-721302, India
[3] Instituto de Ciencias Nucleares, Universidad Nacional Autónoma de Mexico, A.P. 70-543 Mexico 04510 D.F., Mexico

Received: 8 June 2004 / Revised version: 20 September 2004 /
Published online: 4 January 2005 –
Communicated by V. Vento

Abstract. The two-neutrino double-beta decay of ^{94,96}Zr,^{98,100}Mo,^{104}Ru and ^{110}Pd nuclei for the $0^+ \rightarrow 0^+$ transition is studied in the PHFB model in conjunction with the summation method. In the first step, the reliability of the intrinsic wave functions has been established by obtaining an overall agreement between a number of theoretically calculated spectroscopic properties and the available experimental data for ^{94,96}Zr,^{94,96,98,100}Mo, ^{98,100,104}Ru, ^{104,110}Pd and ^{110}Cd isotopes. Subsequently, the PHFB wave functions of the above-mentioned nuclei are employed to calculate the nuclear transition matrix elements $M_{2\nu}$ as well as half-lives $T^{2\nu}_{1/2}$. Furthermore, we have studied the effects of deformation on the $M_{2\nu}$.

PACS. 23.40.Hc Relation with nuclear matrix elements and nuclear structure – 21.60.Jz Hartree-Fock and random-phase approximations – 23.20.-g Electromagnetic transitions – 27.60.+j $90 \leq A \leq 149$

1 Introduction

The implications of present studies about the nuclear double-beta ($\beta\beta$) decay [1,2] are far reaching in Nature. The two-neutrino double-beta (2ν $\beta\beta$) decay is a second-order process of weak interaction and conserves the lepton number exactly. Hence, it is allowed in the standard model of electroweak unification (SM). The half-life of the 2ν $\beta\beta$ decay, which is a product of an accurately known phase space factor and an appropriate nuclear transition matrix element (NTME) $M_{2\nu}$, has been already measured for about ten nuclei out of 35 possible candidates. So, the values of the NTME $M_{2\nu}$ can be extracted directly. Consequently, the validity of different models employed for nuclear-structure calculations can be tested by calculating the $M_{2\nu}$. The neutrinoless double-beta (0ν $\beta\beta$) decay is a convenient tool to test physics beyond the SM. The experimental as well as the theoretical aspect of nuclear $\beta\beta$ decay have been widely reviewed over the past years [3–19].

Klapdor and his group have recently reported that the 0ν $\beta\beta$ decay has been observed in ^{76}Ge. The results are controversial but it is expected that the issue will be settled soon [20]. The aim of all the present experimental activities is to observe the 0ν $\beta\beta$ decay. As the 0ν $\beta\beta$ decay has not been observed so far, the nuclear models predict half-lives assuming certain values for the neutrino mass or conversely extract various parameters from the observed limits on half-lives of the 0ν $\beta\beta$ decay. The reliability of the predictions can be judged *a priori* only from the success of a nuclear model in explaining various observed physical properties of nuclei. The common practice is to calculate the $M_{2\nu}$ to start with and compare them with the experimental value as the two decay modes involve the same set of initial and final nuclear wave functions.

In 2ν $\beta\beta$ decay, the total angular momentum of four S-wave leptons can be 0, 1 or 2, and is equal to the total angular momentum transferred between the parent and daughter nuclei. The lowest 1^+ state in the final nucleus of any $\beta\beta$ decay candidate lies much higher in energy than the first-excited 2^+ state. Hence, the $0^+ \rightarrow 1^+$ transition is much less probable than the $0^+ \rightarrow 0^+$ and $0^+ \rightarrow 2^+$ transitions. Since the $0^+ \rightarrow 2^+$ transition has not been detected up to now, the present theoretical predictions can only be checked against the $0^+ \rightarrow 0^+$ transition of the 2ν $\beta\beta$ decay.

In all cases of the 2ν $\beta\beta$ decay for the $0^+ \rightarrow 0^+$ transition, it is observed that the NTMEs $M_{2\nu}$ are quenched, *i.e.* they are smaller than those predicted for pure quaisparticle transitions. The main objective of all nuclear-structure calculations is to understand the physical mechanism responsible for the suppression of the $M_{2\nu}$. Over the past few years, the $M_{2\nu}$ has been calculated mainly in three types of models, namely the shell model and its variants, the quasiparticle random phase approximation (QRPA) and

[a] e-mail: pkraina@phy.iitkgp.ernet.in

its extensions and the alternative models. In the recent past, the details about these models —their advantages as well as shortcomings— have been discussed by Suhonen *et al.* [12] and Faessler *et al.* [13].

The shell model attempts to solve the nuclear many-body problem as exactly as possible. Hence, it is the best choice for the calculation of the NTMEs. However, most of the $\beta\beta$ decay emitters are medium- or heavy-mass nuclei for which the number of basis states increases quite drastically. A few years back, it was not possible to perform a reliable shell model calculation beyond the *pf*-shell. Hence, Haxton and Stephenson jr. [5] and Vergados [7] have studied the $\beta\beta$ decay of ^{76}Ge, ^{82}Se and ^{128,130}Te nuclei in the weak-coupling limit. Recent large-scale shell model calculations are more promising in nature [21,22]. The calculations by Caurier *et al.* are more realistic in which the $M_{2\nu}$ of ^{82}Se is calculated exactly and those of ^{76}Ge and ^{136}Xe are dealt in a nearly exact manner [22]. The conventional shell model and Monte Carlo shell model (MCSM) [23] have been tested against each other in case of ^{48}Ca and ^{76}Ge and the agreement is interestingly good. Hence, it is expected that the MCSM could be a good alternative to conventional shell model calculations in the near future.

Vogel and Zirnbauer were the first to provide an explanation of the observed suppression of $M_{2\nu}$ in the QRPA model by a proper inclusion of ground-state correlations through the proton-neutron *p*-*p* interaction in the $S = 1$, $T = 0$ channel and the calculated half-lives are in close agreement with all the experimental data [24]. The QRPA frequently overestimates the ground-state correlations as a result of an increase in the strength of attractive proton-neutron interaction leading to the collapse of QRPA solutions. The physical value of this force is usually close to the point at which the QRPA solutions collapse. To cure the strong suppression of $M_{2\nu}$, several extensions of QRPA have been proposed. The most important proposals are inclusion of proton-neutron pairing, renormalized QRPA, higher QRPA, multiple commutator method (MCM) and particle number projection. However, none of the above methods is free from ambiguities [13]. Alternative models, as the operator expansion method (OEM), the broken $SU(4)$ symmetry, two vacua RPA, the pseudo $SU(3)$ and the single state dominance hypothesis (SSDH) have their own problems [12].

The basic aim of nuclear many-body theory is to describe as much observed properties of nuclei as possible in a coherent frame. The $\beta\beta$ decay can be studied in the same framework of many other nuclear properties and decays. Over the past years, a vast amount of data has been collected through experimental studies involving in-beam γ-ray spectroscopy concerning the level energies as well as electromagnetic properties. The availability of data permits a rigorous and detailed critique of the ingredients of the microscopic framework that seeks to provide a description of nuclear $\beta\beta$ decay. However, most of the calculations of $\beta\beta$ decay matrix elements performed so far do not satisfy this criterion. Our aim is to study the 2ν $\beta\beta$ decay of ^{94,96}Zr, ^{98,100}Mo, ^{104}Ru and ^{110}Pd isotopes for the $0^+ \rightarrow 0^+$ transition not in isolation but together with other observed nuclear phenomena. The 2ν $\beta\beta$ decay of ^{100}Mo along with the spectroscopic properties has been already studied in the Projected Hartree-Fock-Bogoliubov (PHFB) model using the closure approximation [25,26]. In the present calculation, we have avoided the closure approximation by making use of the summation method [27]. Further, the HFB wave functions of ^{100}Mo are generated with improved accuracy.

The structure of nuclei in the mass region $A \approx 100$ involving Zr, Mo, Ru, Pd and Cd isotopes is quite complex. With the discovery of a new region of deformation around $A = 100$ by Cheifetz *et al.* [28], a well-developed rotational spectrum was observed in several neutron-rich Mo and Ru isotopes during a study of fission fragments of ^{252}Cf. The $B(E2{:}\ 0^+ \rightarrow 2^+)$ values were observed to be as enhanced as in the rare-earth and actinide regions. This mass region offered a nice example of shape transition, the sudden onset of deformation at neutron number $N = 60$. The nuclei are soft vibrators for the neutron number $N < 60$ and quasirotors for $N > 60$. The nuclei with neutron number $N = 60$ are transitional nuclei. Thus, in this mass region ^{100}Zr, ^{102}Mo, ^{104}Ru and ^{106}Pd are observed to be transitional cases. In case of Cd isotopes, a similar shape transition occurs at $A = 100$. Hence, it is expected that deformation will play a crucial role in reproducing the properties of nuclei in this mass region $A \approx 100$. Moreover, it has been already conjectured that the deformation can play a crucial role in case of $\beta\beta$ decay of ^{100}Mo and ^{150}Nd [29,30]. Further, all the nuclei undergoing $\beta\beta$ decay are of even-even type, in which the pairing degrees of freedom play an important role. Hence, it is desirable to have a model which incorporates the pairing and deformation degrees of freedom on equal footing in its formalism. For this purpose, the PHFB model is one of the most natural choices. However, in the present version of the PHFB model, it is not possible to study the structure of odd-odd nuclei. Hence, the single-beta decay rates and the distribution of Gamow-Teller strength cannot be calculated. On the other hand, the study of these processes has implications in the understanding of the role of the isoscalar part of the proton-neutron interaction. This is a serious drawback in the present formalism of the PHFB model.

Over the past twenty years, extensive studies of shape transition vis-à-vis electromagnetic properties of Zr and Mo isotopes have been successfully carried out in the PHFB model [31] using the pairing plus quadrupole-quadrupole (PPQQ) interaction [32]. The success of the PHFB model in explaining the observed experimental trends in the mass region $A \approx 100$ motivated us to apply the HFB wave functions to study the nuclear 2ν $\beta\beta$ decay of $^{100}\text{Mo} \rightarrow {}^{100}\text{Ru}$ for the $0^+ \rightarrow 0^+$ transition. Further, the success of the PHFB model in conjunction with the PPQQ interaction in explaining the yrast spectra, reduced transition probabilities $B(E2{:}\ 0^+ \rightarrow 2^+)$, static quadrupole moments $Q(2^+)$, g-factors $g(2^+)$ of ^{100}Mo and ^{100}Ru nuclei as well as the $T^{2\nu}_{1/2}(0^+ \rightarrow 0^+)$ of ^{100}Mo [25] has prompted us to apply the PHFB model to study the 2ν $\beta\beta$ decay of some nuclei namely ^{94,96}Zr, ^{98,100}Mo, ^{104}Ru and ^{110}Pd for the $0^+ \rightarrow 0^+$ transition in the mass range $94 \leq A \leq 110$.

It is well known that the pairing part of the interaction (P) accounts for the sphericity of the nucleus, whereas the quadrupole-quadrupole (QQ) interaction increases the collectivity in the nuclear intrinsic wave functions and makes the nucleus deformed. Hence, the PHFB model using the PPQQ interaction is a convenient choice to examine the explicit role of deformation on the NTMEs $M_{2\nu}$. In case of ^{100}Mo for the $0^+ \to 0^+$ transition, we have observed that the deformation plays an important role in reproducing a realistic $M_{2\nu}$ [25]. Therefore, we have also studied the variation of $M_{2\nu}$ vis-à-vis the change in deformation through the changing strength of the QQ interaction.

The present paper has been organized as follows. The theoretical formalism to calculate the half-life of the 2ν $\beta\beta$ decay mode has been given by Haxton and Stephenson jr. [5], Doi *et al.* [6] and Tomoda [9]. Hence in sect. 2, we briefly outline steps of the above derivations for clarity in notations used in the present paper following Doi *et al.* [6]. Further, we have presented formulae to calculate the NTME of the 2ν $\beta\beta$ decay in the PHFB model in conjunction with the summation method. Expressions used to calculate the nuclear spectroscopic properties, namely yrast spectra, reduced $B(E2)$ transition probabilities, static quadrupole moments and g-factors have been given by Dixit *et al.* [25]. In sect. 3.1, as a test of the reliability of the wave functions, we have calculated the yrast spectra, reduced $B(E2{:}\ 0^+ \to 2^+)$ transition probabilities, static quadrupole moments $Q(2^+)$ and g-factors $g(2^+)$ of nuclei participating in the 2ν $\beta\beta$ decay and compared with the available experimental data. Subsequently, the HFB wave functions of the above-mentioned nuclei are employed to calculate the $M_{2\nu}$ as well as half-lives $T^{2\nu}_{1/2}$ in sect. 3.2. In sect. 3.3, the role of deformation on $M_{2\nu}$ has been studied through varying the strength of the QQ interaction. Finally, the conclusions are given in sect. 4.

2 Theoretical framework

The inverse half-life of the 2ν $\beta\beta$ decay for the $0^+ \to 0^+$ transition is given by

$$[T^{2\nu}_{1/2}(0^+ \to 0^+)]^{-1} = G_{2\nu}|M_{2\nu}|^2 \,. \tag{1}$$

The integrated kinematical factor $G_{2\nu}$ can be calculated with good accuracy [6] and the NTME $M_{2\nu}$ is given by

$$M_{2\nu} = \sum_N \frac{\langle 0^+_F||\boldsymbol{\sigma}\tau^+||1^+_N\rangle\langle 1^+_N||\boldsymbol{\sigma}\tau^+||0^+_I\rangle}{E_N - (E_I + E_F)/2} \tag{2}$$

$$= \sum_N \frac{\langle 0^+_F||\boldsymbol{\sigma}\tau^+||1^+_N\rangle\langle 1^+_N||\boldsymbol{\sigma}\tau^+||0^+_I\rangle}{E_0 + E_N - E_I} \,, \tag{3}$$

where

$$E_0 = \frac{1}{2}\,(E_I - E_F) = \frac{1}{2}Q_{\beta\beta} + m_e \tag{4}$$

The summation over intermediate states can be completed using the summation method [27] and the $M_{2\nu}$ can be written as

$$M_{2\nu} = \frac{1}{E_0}\left\langle 0^+_F \left| \sum_m (-1)^m \Gamma_{-m} F_m \right| 0^+_I \right\rangle \,, \tag{5}$$

where the Gamow-Teller (GT) operator Γ_m is given by

$$\Gamma_m = \sum_s \sigma_{ms}\tau^+_s \tag{6}$$

and

$$F_m = \sum_{\lambda=0}^{\infty} \frac{(-1)^\lambda}{E_0^\lambda} D_\lambda \Gamma_m \tag{7}$$

with

$$D_\lambda \Gamma_m = [H, [H, \ldots, [H, \Gamma_m]\ldots]]^{(\lambda \text{ times})} \,. \tag{8}$$

Presently, we have used a Hamiltonian of PPQQ type [32] of the effective two-body interaction, which is explicitly written as

$$H = H_{\rm sp} + V(P) + \chi_{qq} V(QQ) \,, \tag{9}$$

where $H_{\rm sp}$ denotes the single-particle Hamiltonian. The pairing part of the effective two-body interaction $V(P)$ is written as

$$V(P) = -\left(\frac{G}{4}\right) \sum_{\alpha\beta} (-1)^{j_\alpha + j_\beta - m_\alpha - m_\beta} a^\dagger_\alpha a^\dagger_{\bar\alpha} a_{\bar\beta} a_\beta \,, \tag{10}$$

where α denotes the quantum numbers ($nljm$). The state $\bar\alpha$ is the same as α but with the sign of m reversed. The QQ part of the effective interaction $V(QQ)$ is given by

$$V(QQ) = -\left(\frac{\chi}{2}\right) \sum_{\alpha\beta\gamma\delta} \sum_\mu (-1)^\mu \langle\alpha|q^2_\mu|\gamma\rangle\langle\beta|q^2_{-\mu}|\delta\rangle a^\dagger_\alpha a^\dagger_\beta a_\delta a_\gamma, \tag{11}$$

where

$$q^2_\mu = \left(\frac{16\pi}{5}\right)^{1/2} r^2 Y^2_\mu(\theta, \phi) \,. \tag{12}$$

The χ_{qq} is an arbitrary parameter and the final results are obtained by setting the $\chi_{qq} = 1$. The purpose of introducing χ_{qq} is to study the role of deformation by varying the strength of the QQ interaction.

When the GT operator commutes with the effective two-body interaction, eq. (8) can be further simplified to

$$M_{2\nu} = \sum_{\pi,\nu} \frac{\langle 0^+_F||\boldsymbol{\sigma}\cdot\boldsymbol{\sigma}\tau^+\tau^+||0^+_I\rangle}{E_0 + \varepsilon(n_\pi, l_\pi, j_\pi) - \varepsilon(n_\nu, l_\nu, j_\nu)} \,. \tag{13}$$

In the case of the pseudo-$SU(3)$ model [33–35], the GT operator commutes with the two-body interaction and the energy denominator is a well-defined quantity without any free parameter. It has been evaluated exactly for 2ν $\beta^-\beta^-$ [33,34] and 2ν ECEC modes [35] in the context of the pseudo-$SU(3)$ scheme. In the present case, the model Hamiltonian is not isospin symmetric. Hence, the energy denominator has not the simple form shown in eq. (13).

However, the violation of isospin symmetry for the QQ part of our model Hamiltonian is negligible as will be evident from the parameters of the two-body interaction given later. Also the violation of isospin symmetry for the pairing part of the two-body interaction is presumably small. With these assumptions, the expression to calculate the NTME $M_{2\nu}$ of the 2ν $\beta\beta$ decay for the $0^+ \rightarrow 0^+$ transition in the PHFB model is obtained as follows.

The axially symmetric HFB intrinsic state with $K = 0$ can be written as

$$|\Phi_0\rangle = \prod_{im}(u_{im} + v_{im} b^\dagger_{im} b^\dagger_{i\bar{m}})|0\rangle \ , \tag{14}$$

where the creation operators $b^\dagger_{im}$ and $b^\dagger_{i\bar{m}}$ are given by

$$\begin{aligned} b^\dagger_{im} &= \sum_\alpha C_{i\alpha,m} a^\dagger_{\alpha m} \qquad \text{and} \\ b^\dagger_{i\bar{m}} &= \sum_\alpha (-1)^{l+j-m} C_{i\alpha,m} a^\dagger_{\alpha,-m} \ . \end{aligned} \tag{15}$$

Using the standard projection technique, a state with good angular momentum $\mathbf{J}$ is obtained from the HFB intrinsic state through the following relation:

$$\begin{aligned} |\Psi^J_{MK}\rangle &= P^J_{MK}|\Phi_K\rangle \\ &= \left[\frac{(2J+1)}{8\pi^2}\right] \int D^J_{MK}(\Omega) R(\Omega) |\Phi_K\rangle \mathrm{d}\Omega \ , \end{aligned} \tag{16}$$

where $R(\Omega)$ and $D^J_{MK}(\Omega)$ are the rotation operator and the rotation matrix, respectively.

Finally, one obtains the following expression for the NTME $M_{2\nu}$ of the 2ν $\beta\beta$ decay for the $0^+ \rightarrow 0^+$ transition in the PHFB model using the summation method:

$$\begin{aligned} M_{2\nu} &= \sum_{\pi,\nu} \frac{\langle \Psi^{J_f=0}_{00} || \boldsymbol{\sigma} \cdot \boldsymbol{\sigma} \tau^+ \tau^+ || \Psi^{J_i=0}_{00} \rangle}{E_0 + \varepsilon(n_\pi, l_\pi, j_\pi) - \varepsilon(n_\nu, l_\nu, j_\nu)} \\ &= \left[n^{Ji=0}_{(Z,N)} n^{J_f=0}_{(Z+2,N-2)} \right]^{-1/2} \int_0^\pi n_{(Z,N),(Z+2,N-2)}(\theta) \\ &\quad \times \sum_{\alpha\beta\gamma\delta} \frac{\langle \alpha\beta \,|\boldsymbol{\sigma}_1 \cdot \boldsymbol{\sigma}_2 \tau^+ \tau^+| \, \gamma\delta \rangle}{E_0 + \varepsilon_\alpha(n_\pi, l_\pi, j_\pi) - \varepsilon_\gamma(n_\nu, l_\nu, j_\nu)} \\ &\quad \times \sum_{\varepsilon\eta} \left[\left(1 + F^{(\pi)}_{Z,N}(\theta) f^{(\pi)*}_{Z+2,N-2} \right) \right]^{-1}_{\varepsilon\alpha} \left(f^{(\pi)*}_{Z+2,N-2} \right)_{\varepsilon\beta} \\ &\quad \times \left[\left(1 + F^{(\nu)}_{Z,N}(\theta) f^{(\nu)*}_{Z+2,N-2} \right) \right]^{-1}_{\gamma\eta} \left(F^{(\nu)*}_{Z,N} \right)_{\eta\delta} \sin\theta \mathrm{d}\theta \ , \end{aligned} \tag{17}$$

where

$$\begin{aligned} n^J &= \int_0^\pi \left[\det \left(1 + F^{(\pi)} f^{(\pi)^\dagger} \right) \right]^{1/2} \\ &\quad \times \left[\det \left(1 + F^{(\nu)} f^{(\nu)^\dagger} \right) \right]^{1/2} d^J_{00}(\theta) \sin(\theta) \mathrm{d}\theta \end{aligned}$$

and

$$\begin{aligned} n_{(Z,N),(Z+2,N-2)}(\theta) &= \left[\det \left(1 + F^{(\nu)}_{Z,N} f^{(\nu)^\dagger}_{Z+2,N-2} \right) \right]^{1/2} \\ &\quad \times \left[\det \left(1 + F^{(\pi)}_{Z,N} f^{(\pi)^\dagger}_{Z+2,N-2} \right) \right]^{1/2} . \end{aligned} \tag{18}$$

The π (ν) represents the proton (neutron) of nuclei involved in the 2ν $\beta\beta$ decay process. The matrices $F_{Z,N}(\theta)$ and $f_{Z,N}$ are given by

$$F_{Z,N}(\theta) = \sum_{m'_\alpha m'_\beta} d^{j_\alpha}_{m_\alpha, m'_\alpha}(\theta) d^{j_\beta}_{m_\beta, m'_\beta}(\theta) f_{j_\alpha m'_\alpha, j_\beta m'_\beta} \ , \tag{19}$$

$$f_{Z,N} = \sum_i C_{ij_\alpha, m_\alpha} C_{ij_\beta, m_\beta} \left(v_{im_\alpha} / u_{im_\alpha} \right) \delta_{m_\alpha, -m_\beta} \ . \tag{20}$$

The required NTME $M_{2\nu}$ is calculated using the results of PHFB calculations which are summarized by the amplitudes (u_{im}, v_{im}) and the expansion coefficients $C_{ij,m}$. In the first step, matrices $F^{\pi,\nu}$ and $f^{\pi,\nu}$ are set up for the nuclei involved in the 2ν $\beta\beta$ decay making use of 20 Gaussian quadrature points in the range $(0, \pi)$. Finally using eq. (17), the required NTME can be calculated in a straightforward manner.

3 Results and discussions

The model space, single-particle energies (SPEs) and two-body interactions are the same as in our earlier calculation on the 2ν $\beta\beta$ decay of ^{100}Mo for the $0^+ \rightarrow 0^+$ transition [25]. However, we have included a brief discussion of them in the following for convenience. We have treated the doubly even nucleus ^{76}Sr ($N = Z = 38$) as an inert core with the valence space spanned by orbits $1p_{1/2}$, $2s_{1/2}$, $1d_{3/2}$, $1d_{5/2}$, $0g_{7/2}$, $0g_{9/2}$ and $0h_{11/2}$ for protons and neutrons. The orbit $1p_{1/2}$ has been included in the valence space to examine the role of the $Z = 40$ proton core vis-à-vis the onset of deformation in the highly neutron-rich isotopes.

The set of single-particle energies (SPEs) used here is (in MeV) $\varepsilon(1p_{1/2}) = -0.8$, $\varepsilon(0g_{9/2}) = 0.0$, $\varepsilon(1d_{5/2}) = 5.4$, $\varepsilon(2s_{1/2}) = 6.4$, $\varepsilon(1d_{3/2}) = 7.9$, $\varepsilon(0g_{7/2}) = 8.4$ and $\varepsilon(0h_{11/2}) = 8.6$ for protons and neutrons. This set of SPEs but for the $\varepsilon(0h_{11/2})$, which is slightly lowered, has been employed in a number of successful shell model [36] as well as variational-model calculations [31] for nuclear properties in the mass region $A = 100$. The strengths of the pairing interaction is fixed through the relations $G_p = 30/A$ MeV and $G_n = 20/A$ MeV, which are the same used by Heestand *et al.* [37] to explain the experimental $g(2^+)$ data of some even-even Ge, Se, Mo, Ru, Pd, Cd and Te isotopes in Greiner's collective model [38]. For ^{96}Zr, we have used $G_n = 22/A$ MeV. The strengths of the like-particle components of the QQ interaction are taken as: $\chi_{pp} = \chi_{nn} = 0.0105$ MeV b^{-4}, where b is the oscillator parameter.

The strength of the proton-neutron (pn) component of the QQ interaction χ_{pn} is varied so as to obtain the spectra of the considered nuclei namely ^{94,96}Zr, ^{94,96,98,100}Mo,

Table 1. Excitation energies (in MeV) of $J^\pi = 2^+$, 4^+, 6^+ yrast states of some nuclei in the mass range $94 \leq A \leq 110$ with fixed $G_p = 30/A$, $G_n = 20/A$ ($22/A$ for ^{96}Zr) and $\varepsilon(h_{11/2}) = 8.6$ MeV.

Nucleus	χ_{pn}	Theory		Experiment [40]	Nucleus	χ_{pn}	Theory		Experiment [40]
^{94}Zr	0.02519	E_{2+}	0.9182	0.9183	^{94}Mo	0.02670	E_{2+}	0.8715	0.871099
		E_{4+}	1.9732	1.4688			E_{4+}	1.9685	1.573726
		E_{6+}	2.7993				E_{6+}	3.3136	2.42337
^{96}Zr	0.01717	E_{2+}	1.7570	1.7507	^{96}Mo	0.02557	E_{2+}	0.7779	0.778213
		E_{4+}	3.5269	3.1202			E_{4+}	2.0373	1.62815
		E_{6+}	9.7261				E_{6+}	3.5776	2.44064
^{98}Mo	0.01955	E_{2+}	0.7892	0.78742	^{98}Ru	0.02763	E_{2+}	0.6513	0.65241
		E_{4+}	1.9522	1.51013			E_{4+}	1.9430	1.3978
		E_{6+}	3.3098	2.3438			E_{6+}	3.6548	2.2227
^{100}Mo	0.01906	E_{2+}	0.5356	0.53555	^{100}Ru	0.01838	E_{2+}	0.5395	0.53959
		E_{4+}	1.4719	1.13594			E_{4+}	1.5591	1.2265
		E_{6+}	2.6738				E_{6+}	2.8940	2.0777
^{104}Ru	0.02110	E_{2+}	0.3580	0.35799	^{104}Pd	0.01486	E_{2+}	0.5552	0.55579
		E_{4+}	1.1339	0.8885			E_{4+}	1.5729	1.32359
		E_{6+}	2.2280	1.5563			E_{6+}	2.8790	2.2498
^{110}Pd	0.01417	E_{2+}	0.3737	0.3738	^{110}Cd	0.01412	E_{2+}	0.6576	0.657751
		E_{4+}	1.1563	0.9208			E_{4+}	1.8709	1.542412
		E_{6+}	2.2254	1.5739			E_{6+}	3.3865	2.479893

^{98,100,104}Ru, ^{104,110}Pd and ^{110}Cd in optimum agreement with the experimental results. To be more specific, we have taken the theoretical spectra to be the optimum if the excitation energy of the 2^+ state E_{2^+} is reproduced as closely as possible to the experimental value. Thus, for a given model space, SPEs, G_p, G_n and χ_{pp}, we have fixed χ_{pn} through the experimentally available energy spectra. We have given the values of χ_{pn} in table 1. These values for the strength of the QQ interaction are comparable to those suggested by Arima on the basis of an empirical analysis of the effective two-body interactions [39]. All the parameters are kept fixed throughout the calculation.

3.1 The yrast spectra and electromagnetic properties

In table 1, we have presented yrast energies for E_{2^+}-to- E_{6^+} levels of all nuclei of interest. The agreement between the theoretically reproduced E_{2^+} and the experimentally observed E_{2^+} [40] is quite good. However, it is observed that in comparison to the experimental spectra, the theoretical spectra are more expanded. This can be corrected to some extent in the PHFB model in conjunction with the VAP prescription [31]. However, our aim is to reproduce properties of the low-lying 2^+ state. Hence, we have not attempted to invoke the VAP prescription, which will unnecessarily complicate the calculations.

In table 2 we have presented the calculated as well as the experimentally observed values of the reduced transition probabilities $B(E2{:}\ 0^+ \to 2^+)$ [41], static quadrupole moments $Q(2^+)$ and the gyromagnetic factors $g(2^+)$ [42]. We have given the $B(E2{:}\ 0^+ \to 2^+)$ results for effective charges $e_{\rm eff} = 0.40$, 0.50 and 0.60 in columns 2 to 4, respectively. The experimentally observed values are displayed in column 5. In case of $B(E2{:}\ 0^+ \to 2^+)$, only some experimentally observed representative values are tabulated. It is noticed that the calculated values are in excellent agreement with the observed $B(E2{:}\ 0^+ \to 2^+)$ in case of ^{94}Zr, ^{94,100}Mo, ^{100,104}Ru and ^{104}Pd nuclei for $e_{\rm eff} = 0.60$. The calculated and observed $B(E2{:}\ 0^+ \to 2^+)$ values are again in agreement in case of ^{96}Zr and ^{96}Mo nuclei for $e_{\rm eff} = 0.50$. The calculated $B(E2{:}\ 0^+ \to 2^+)$ values for $e_{\rm eff} = 0.50$ differ by 0.046 and 0.004 e^2b^2 only in case of ^{110}Pd and ^{110}Cd nuclei, respectively, from the experimental limits. The agreement between the theoretical and experimental $B(E2{:}\ 0^+ \to 2^+)$ values is quite good in case of ^{98}Mo and ^{98}Ru nuclei for $e_{\rm eff} = 0.40$.

The theoretically calculated $Q(2^+)$ are tabulated in columns 6 to 8 for the same effective charges as given above. The experimental $Q(2^+)$ results are given in column 9. No experimental $Q(2^+)$ result is available for ^{94,96}Zr. It can be seen that for the same effective charge as used in case of $B(E2{:}\ 0^+ \to 2^+)$, the agreement between the calculated and experimental $Q(2^+)$ values is quite good for ^{104}Ru and ^{110}Pd nuclei. The discrepancy between the calculated and experimental values is off by 0.089, 0.14 and 0.023 e b in case of ^{98,100}Mo and ^{100}Ru nuclei, respectively. The theoretical $Q(2^+)$ results are quite off from the observed values for the rest of nuclei.

The $g(2^+)$ values are calculated with $g_l^\pi = 1.0$, $g_l^\nu = 0.0$, $g_s^\pi = g_s^\nu$=0.60. No experimental result is available for ^{96}Zr and ^{94,96}Mo. The calculated and experimentally observed $g(2^+)$ are in good agreement for ^{98,100}Mo, ^{98}Ru, ^{104}Pd and ^{110}Cd nuclei. The discrepancy between the theoretically calculated and experimentally observed $g(2^+)$ values is 0.035, 0.021 and 0.078 nm only

Table 2. Comparison of calculated and experimentally observed reduced transition probabilities $B(E2;\ 0^+ \to 2^+)$ in $e^2\,b^2$, static quadrupole moments $Q(2^+)$ in e b and g-factors $g(2^+)$ in nuclear magneton. Here $B(E2)$ and $Q(2^+)$ are calculated for effective charge $e_p = 1 + e_{\rm eff}$ and $e_n = e_{\rm eff}$. $g(2^+)$ has been calculated for $g_l^\pi = 1.0$, $g_l^\nu = 0.0$ and $g_s^\pi = g_s^\nu = 0.60$.

Nucleus	$B(E2;\ 0^+ \to 2^+)$				$Q(2^+)$				$g(2^+)$	
	Theory $e_{\rm eff}$			Experiment[a]	Theory $e_{\rm eff}$			Experiment[b]	Theory	Experiment[b]
	0.40	0.50	0.60		0.40	0.50	0.60			
^{94}Zr	0.046	0.062	**0.081**	0.081±0.017	−0.168	−0.195	**−0.222**		0.121	−0.329±0.015[c]
				0.066 ± 0.014						−0.26±0.06
				0.056 ± 0.014						−0.05±0.05
^{94}Mo	0.148	0.188	**0.232**	0.230±0.040	−0.347	−0.391	**−0.435**	−0.13±0.08	0.343	
				0.270 ± 0.035						
				0.290 ± 0.044						
^{96}Zr	0.044	**0.060**	0.078	0.055±0.022	−0.012	**−0.015**	−0.018		0.254	
^{96}Mo	0.265	**0.335**	0.413	0.310±0.047	−0.466	**−0.524**	−0.582	−0.20 ± 0.08	0.563	
				0.302 ± 0.039						
				0.288 ± 0.016						
^{98}Mo	**0.234**	0.302	0.378	0.260±0.040	**−0.439**	−0.498	−0.557	−0.26 ± 0.09	0.376	0.34 ± 0.18
				0.270 ± 0.040						
				0.267 ± 0.005						
^{98}Ru	**0.433**	0.543	0.665	0.411±0.035	**−0.596**	−0.667	−0.739	−0.20 ± 0.09	0.528	0.39 ± 0.30
				0.475 ± 0.038				−0.03 ± 0.14		
				0.392 ± 0.012						
^{100}Mo	0.320	0.412	**0.515**	0.511±0.009	−0.512	−0.581	**−0.650**	−0.42 ± 0.09	0.477	0.34 ± 0.18
				0.516 ± 0.010				−0.39 ± 0.08		
				0.470 ± 0.024						
^{100}Ru	0.308	0.393	**0.488**	0.494±0.006	−0.503	−0.568	**−0.633**	−0.54 ± 0.07	0.355	0.42 ± 0.03
				0.493 ± 0.003				−0.40 ± 0.12		0.47 ± 0.06
				0.501 ± 0.010				−0.43 ± 0.07		
^{104}Ru	0.572	0.732	**0.912**	0.93±0.06	−0.684	−0.774	**−0.864**	−0.76 ± 0.19	0.339	0.41 ± 0.05
				1.04 ± 0.16				−0.70 ± 0.08		
				0.841 ± 0.016				−0.66 ± 0.05		
^{104}Pd	0.361	0.460	**0.571**	0.547±0.038	−0.543	−0.613	**−0.682**	−0.47 ± 0.10	0.439	0.46 ± 0.04
				0.61 ± 0.09						0.40±0.05
				0.535 ± 0.035						0.38±0.04
^{110}Pd	0.479	**0.614**	0.766	0.780±0.120	−0.626	**−0.708**	−0.791	−0.72 ± 0.14	0.478	0.37 ± 0.03
				0.820 ± 0.080				−0.55 ± 0.08		0.35 ± 0.03
				0.860 ± 0.060				−0.47 ± 0.03		0.31 ± 0.03
^{110}Cd	0.427	**0.548**	0.685	0.504±0.040	−0.590	**−0.668**	−0.746	−0.40 ± 0.04	0.358	0.31 ± 0.07
				0.467 ± 0.019				−0.39 ± 0.06		0.28 ± 0.05
				0.450 ± 0.020				−0.36 ± 0.08		0.285 ± 0.055

([a]) Reference [41].
([b]) Reference [42].
([c]) Reference [43].

for ^{100,104}Ru and ^{110}Pd nuclei, respectively. The theoretical $g(2^+)$ value of ^{94}Zr is a pathological case. The calculated $g(2^+)$ value is 0.121 nm while the most recent measured value is -0.329 ± 0.015 nm [43].

From the overall agreement between the calculated and observed electromagnetic properties, it is clear that the PHFB wave functions of ^{94,96}Zr, ^{94,96,98,100}Mo, ^{98,100,104}Ru, ^{104,110}Pd and ^{110}Cd nuclei generated by fixing χ_{pn} to reproduce the yrast spectra are quite reliable. Hence, we proceed to calculate the NTMEs $M_{2\nu}$ as well as half-lives $T^{2\nu}_{1/2}$ of ^{94,96}Zr, ^{98,100}Mo, ^{104}Ru and ^{110}Pd nuclei for the $0^+ \to 0^+$ transition.

3.2 Results of the $2\nu\ \beta\beta$ decay

The phase space factors $G_{2\nu}$ for the $0^+ \to 0^+$ transition have been given by Boehm *et al.* for $g_A = 1.25$ [10]. These $G_{2\nu}$ are 2.304×10^{-21}, 1.927×10^{-17}, 9.709×10^{-29}, 9.434×10^{-18}, 9.174×10^{-21} and 3.984×10^{-19} y^{-1} for ^{94,96}Zr, ^{98,100}Mo, ^{104}Ru and ^{110}Pd nuclei, respectively. However, in heavy nuclei it is more justified to use the nuclear matter value of g_A around 1.0. Hence, the experimental $M_{2\nu}$ as well as the theoretical $T^{2\nu}_{1/2}$ are calculated for $g_A = 1.0$ and 1.25.

Table 3. Experimentally observed and theoretically calculated $M_{2\nu}$ and half-lives $T^{2\nu}_{1/2}$ for the the $0^+ \to 0^+$ transition of ^{94,96}Zr, ^{98,100}Mo, ^{104}Ru and ^{110}Pd nuclei in different nuclear models. The numbers corresponding to (a) and (b) are calculated for $g_A = 1.25$ and 1.0, respectively.

Nuclei	Experiment					Theory				
	Ref.	Projects	$T^{2\nu}_{1/2}$ (y)		$\lvert M_{2\nu}\rvert$	Ref.	Models	$\lvert M_{2\nu}\rvert$		$T^{2\nu}_{1/2}$ (y)
^{94}Zr	[44]	NEMO	$> 1.1\times10^{-5}$	(a)	< 62.815	*	PHFB	0.076	(a)	7.51
(10^{22} y)				(b)	< 98.148				(b)	18.34
						[47]	SRQRPA			3.08–659
						[46]	OEM			168
						[45]	QRPA			6.93
^{96}Zr	[50]	†gch.	0.94 ± 0.32	(a)	$0.074^{+0.017}_{-0.010}$	*	PHFB	0.058	(a)	1.56
(10^{19} y)				(b)	$0.116^{+0.027}_{-0.016}$				(b)	3.80
	[44]	NEMO	$2.1^{+0.8}_{-0.4}\pm0.2$	(a)	$0.050^{+0.009}_{-0.009}$	[47]	SRQRPA			0.452–61
				(b)	$0.078^{+0.014}_{-0.014}$	[56]	$SU(4)_{\sigma\tau}$	0.0678	(a)	1.13
	[49]	NEMO	$2.0^{+0.9}_{-0.5}\pm0.5$	(a)	$0.051^{+0.021}_{-0.012}$				(b)	2.76
				(b)	$0.080^{+0.033}_{-0.019}$	[55]	RQRPA(WS)			4.2
	[48]	†gch.	3.9 ± 0.9	(a)	$0.036^{+0.005}_{-0.004}$	[55]	RQRPA(AWS)			4.4
				(b)	$0.057^{+0.008}_{-0.006}$	[54]	QRPA(AWS)	0.12–0.31	(a)	0.054–0.36
	[18]	Average	$1.4^{+3.5}_{-0.5}$	(a)	$0.061^{+0.015}_{-0.028}$				(b)	0.13–0.88
		value		(b)	$0.095^{+0.024}_{-0.044}$	[53]	SRPA(WS)	0.022	(a)	10.72
	[51]	Recommended	$2.1^{+0.8}_{-0.4}$	(a)	$0.050^{+0.006}_{-0.007}$				(b)	26.18
		value		(b)	$0.078^{+0.009}_{-0.012}$	[46]	OEM			20.2
						[45]	QRPA			1.08
						[52]	QRPA	0.124	(a)	0.34
									(b)	0.82
^{98}Mo						*	PHFB	0.130	(a)	6.09
(10^{29} y)									(b)	14.87
						[47]	SRQRPA			4.06–15.2
						[46]	OEM			61.6
						[45]	QRPA			29.6

In table 3, we have compiled all the available experimental and the theoretical results along with our calculated $M_{2\nu}$ and corresponding half-lives $T^{2\nu}_{1/2}$ of ^{94,96}Zr, ^{98,100}Mo, ^{104}Ru and ^{110}Pd isotopes for the $0^+ \to 0^+$ transition. We have also presented the $M_{2\nu}$ extracted from the experimentally observed $T^{2\nu}_{1/2}$ in column 5 of table 3 using the given phase space factors. We have presented only the theoretical $T^{2\nu}_{1/2}$ for those models for which no direct or indirect information about $M_{2\nu}$ is available to us.

The 2ν $\beta\beta$ decay of $^{94}\text{Zr} \to {}^{94}\text{Mo}$ for the $0^+ \to 0^+$ transition has been investigated experimentally only by Arnold [44], who reported the limit $T^{2\nu}_{1/2} > 1.1\times10^{17}$ y. Theoretical calculations have been done by employing QRPA [45], OEM [46], and SRQRPA [47]. The presently calculated half-life in the PHFB model for $g_A = 1.25$ is 7.51×10^{22} y, which is closer to the value obtained in the QRPA model of Staudt *et al.* [45] and approximately twice the lower limit given by Bobyk *et al.* [47]. On the other hand, the calculated half-life $T^{2\nu}_{1/2}$ in OEM by Hirsch *et al.* [46] is larger than our PHFB model value for $g_A = 1.25$ by a factor of 22 approximately. The predicted $T^{2\nu}_{1/2}$ in the PHFB model for $g_A = 1.0$ is 1.834×10^{23} y.

In case of ^{96}Zr, all the available experimental [18,44, 48–51] and theoretical results [45–47,52–56] along with our calculated $M_{2\nu}$ and corresponding $T^{2\nu}_{1/2}$ are compiled in table 3. In comparison to the experimental $M_{2\nu}$, the theoretically calculated value given by Stoica using SRPA(WS) [53] is too small. On the other hand, the calculated half-life $T^{2\nu}_{1/2}$ in OEM [46] is quite off from the observed experimental value. The $M_{2\nu}$ calculated by Engel *et al.* using QRPA [52] and Barabash *et al.* [54] using QRPA (AWS) for $g_A = 1.0$ is close to the experimentally observed lower limit of Wieser *et al.* [50]. The $T^{2\nu}_{1/2}$ calculated by Toivanen *et al.* in RQRPA (WS) and RQRPA (AWS) are 4.2×10^{19} y and 4.4×10^{19} y [55], respectively and they are quite close to the experimental value of Kawashima *et al.* [48]. The predicted half-life $T^{2\nu}_{1/2}$ of Bobyk *et al.* [47] has a wide range and favors all the available experimental results. On the other hand, the $T^{2\nu}_{1/2}$ predicted by Staudt *et al.* [45] is in agreement with the experimental result of Barabash [49] and Wieser *et al.* [50]. However, the $T^{2\nu}_{1/2}$ calculated in the PHFB model and in $SU(4)_{\sigma\tau}$ by Rumyantsev *et al.* [56] favor the experimental values of NEMO [44, 49] and Wieser *et al.*[50] for $g_A = 1.25$.

In case of $^{98}\text{Mo} \to {}^{98}\text{Ru}$, no experimental result for $T^{2\nu}_{1/2}$ is available so far. The theoretical calculations have been carried out in QRPA [45], OEM [46] and SRQRPA [47]. The calculated $T^{2\nu}_{1/2}$ for $g_A = 1.25$ in

Table 3. Continued.

Nuclei	Experiment					Theory				
	Ref.	Projects	$T^{2\nu}_{1/2}$ (y)		$\lvert M_{2\nu}\rvert$	Ref.	Models	$\lvert M_{2\nu}\rvert$		$T^{2\nu}_{1/2}$ (y)
^{100}Mo	[65]	ITEP+INFN	$7.2 \pm 0.9 \pm 1.8$	(a)	$0.121^{+0.032}_{-0.018}$	*	PHFB	0.104	(a)	9.79
(10^{18} y)				(b)	$0.190^{+0.050}_{-0.028}$				(b)	23.90
	[64]	ITEP	8.5	(a)	0.112	[68]	SSDH		(a)	7.15–8.97
				(b)	0.174	[47]	SRQRPA			5.04–16800
	[63]	UC-Irvine	$6.82^{+0.38}_{-0.53} \pm 0.68$	(a)	$0.125^{+0.013}_{-0.009}$	[56]	$SU(4)_{\sigma\tau}$	0.1606	(a)	4.11
				(b)	$0.195^{+0.020}_{-0.014}$				(b)	10.03
	[62]	LBL+MHC+	$7.6^{+2.2}_{-1.4}$	(a)	$0.118^{+0.013}_{-0.014}$	[67]	SSDH	0.18	(a)	3.27
		UNM+INEL		(b)	$0.185^{+0.020}_{-0.022}$				(b)	7.99
	[61]	NEMO	$9.5 \pm 0.4 \pm 0.9$	(a)	$0.106^{+0.008}_{-0.007}$	[53]	SRPA(WS)	0.059	(a)	30.45
				(b)	$0.165^{+0.013}_{-0.010}$				(b)	74.34
	[60]	LBL	9.7 ± 4.9	(a)	$0.105^{+0.044}_{-0.019}$	[66]	$SU(3)$(SPH)	0.152	(a)	4.59
				(b)	$0.163^{+0.069}_{-0.030}$				(b)	11.2
	[59]	ELEGANTS V	$11.5^{+3.0}_{-2.0}$	(a)	$0.096^{+0.010}_{-0.011}$	[66]	$SU(3)$(DEF)	0.108	(a)	9.09
				(b)	$0.150^{+0.015}_{-0.016}$				(b)	22.19
	[58]	UC-Irvine	$11.6^{+3.4}_{-0.8}$	(a)	$0.096^{+0.004}_{-0.012}$	[46]	OEM			35.8
				(b)	$0.149^{+0.005}_{-0.018}$	[30]	QRPA(EMP)	0.101	(a)	10.39
	[57]	INS Baksan	$3.3^{+2.0}_{-1.0}$	(a)	$0.179^{+0.036}_{-0.038}$				(b)	25.37
				(b)	$0.280^{+0.055}_{-0.059}$	[29]	QRPA(EMP)	0.256	(a)	1.62
	[18]	Average	8.0 ± 0.6	(a)	$0.115^{+0.005}_{-0.004}$				(b)	3.95
		value		(b)	$0.180^{+0.007}_{-0.006}$	[45]	QRPA			1.13
	[51]	Average	8.0 ± 0.7	(a)	$0.115^{+0.005}_{-0.005}$	[52]	QRPA	0.211	(a)	2.38
		value		(b)	$0.180^{+0.008}_{-0.007}$				(b)	5.81
^{104}Ru						*	PHFB	0.068	(a)	2.35
(10^{22} y)									(b)	5.73
						[46]	OEM			3.09
						[45]	QRPA			0.629
^{110}Pd	[69]		$> 6.0 \times 10^{-4}$	(a)	< 6.468	*	PHFB	0.133	(a)	1.41
(10^{20} y)				(b)	< 10.106				(b)	3.44
						[71]	SSDH			1.6
						[67]	SSDH	0.19	(a)	0.7
									(b)	1.70
						[70]	SRPA(WS)	0.046	(a)	11.86
									(b)	28.96
						[46]	OEM			12.4
						[45]	QRPA			0.116

† gch. denotes geochemical experiment.

* Present work.

the PHFB model is in the range given by Bobyk *et al.* in the SRQRPA model [47]. In the PHFB model for $g_A = 1.0$, the predicted half-life of the $2\nu\ \beta\beta$ decay $T^{2\nu}_{1/2}$ is 1.49×10^{30} y. The predicted $T^{2\nu}_{1/2}$ in QRPA by Staudt *et al.* [45] and in OEM by Hirsch *et al.* [46] are larger than our predicted value for $g_A = 1.0$ by approximately a factor of 2 and 4, respectively.

The $2\nu\ \beta\beta$ decay of ^{100}Mo for the $0^+ \to 0^+$ transition has been investigated by many experimental groups [18, 51,57–65] as well as theoreticians by employing different theoretical frameworks[29,30,45–47,52,53,56,66–68]. In comparison to the experimental $M_{2\nu}$, the theoretically calculated value given by Stoica using SRPA(WS) [53] is too small. The $2\nu\ \beta\beta$ decay rate of ^{100}Mo calculated by Staudt *et al.* [45] and Hirsch *et al.* using OEM [46] are off from the experimental $T^{2\nu}_{1/2}$. For $g_A = 1.0$, the $M_{2\nu}$ calculated by Griffiths *et al.* [29] using QRPA model favors the results of INS Baksan [57] and LBL [60] due to the large error bar in the experimental $T^{2\nu}_{1/2}$. On the other hand, the $M_{2\nu}$ predicted by Engel *et al.* [52] and Civitarese *et al.* [67] for $g_A = 1.0$ are in agreement with the results of LBL [60], LBL Collaboration [62], UC-Irvine [63] and ITEP+INFN [65] due to experimental error bars. The values of $M_{2\nu}$ predicted in $SU(4)_{\sigma\tau}$ [56] and $SU3$(SPH) [66] are nearly identical and close to the experimental result given by Vasilev *et al.* [57] and ITEP+INFN [65] for $g_A = 1.25$. The same two $M_{2\nu}$ for $g_A = 1.0$ are in agreement with the results of UC-Irvine [58], ELEGANTS V, LBL and NEMO. Further, the value of $M_{2\nu}$ given by the PHFB model, Suhonen *et al.* using QRPA(EMP) [30]

and Hirsch *et al.* using SU3(DEF) [66] favor the results of UC-Irvine (results of Elliott *et al.*) [58], ELEGANTS V [59], LBL [60], NEMO [61], LBL Collaboration [62] and ITEP+INFN [65] for $g_A = 1.25$. The results of SSDH [68] are in agreement with the experimental half-lives of LBL [60], NEMO [61], LBL Collaboration [62], UC-Irvine [63] and ITEP+INFN [65]. The $T^{2\nu}_{1/2}$ calculated by Bobyk *et al.* [47] is in agreement with all the experimental results due to a large range of values $(5.04–16800)\times10^{18}$ y.

The 2ν $\beta\beta$ decay of ^{104}Ru $\to$ ^{104}Pd for the $0^+ \to 0^+$ transition has not been experimentally investigated so far. The theoretical calculations have been carried out in QRPA [45] and OEM [46]. The predicted $T^{2\nu}_{1/2}$ in QRPA by Staudt *et al.* [45] is approximately one-fourth of our PHFB model prediction for $g_A = 1.25$, while the half-life predicted by Hirsch *et al.* in OEM [46] is approximately 1.31 times larger. We predict a $T^{2\nu}_{1/2}$ for ^{104}Ru to be 5.73×10^{22} y for $g_A = 1.0$.

The 2ν $\beta\beta$ decay of ^{110}Pd $\to$ ^{110}Cd for the $0^+ \to 0^+$ transition has been investigated experimentally by Winter only [69] long back and theoretically by employing QRPA [45], OEM [46], SRPA(WS) [70] and SSDH [67,71]. The $\beta\beta$ decay of the ^{110}Pd $\to$ ^{110}Cd transition was studied by Winter [69] deducing a half-life $T^{2\nu}_{1/2} > 6.0 \times 10^{16}$ y for the 2ν $\beta\beta$ decay mode and a total half-life $> 6.0 \times 10^{17}$ y for all modes. The calculated $T^{2\nu}_{1/2}$ for $g_A = 1.25$ in the present PHFB model is 1.41×10^{20} y, which is close to those of Semenov *et al.* [71] 1.6×10^{20} y and twice that of Civitarese *et al.* [67] 0.7×10^{20} y in SSDH. On the other hand, the calculated half-life by Stoica [70] in SRPA(WS) is 1.186×10^{21} y for the same g_A. The calculated average half-life by Staudt *et al.* [45] in QRPA is 1.16×10^{19} y and by Hirsch *et al.* [46] is 1.24×10^{21} y. For $g_A = 1.0$, we predict a $T^{2\nu}_{1/2}$ for ^{110}Pd to be 3.44×10^{20} y.

It is clear from the above discussions that the validity of nuclear models presently employed to calculate the NTMEs $M_{2\nu}$ as well as half-lives $T^{2\nu}_{1/2}$ cannot be uniquely established due to large error bars in the experimental results as well as uncertainty in g_A. Further work is necessary both in the experimental as well as theoretical front to judge the relative applicability, success and failure of various nuclear models used so far for the study of 2ν $\beta\beta$ decay processes.

3.3 Deformation effect

Out of several possibilities, we have taken the intrinsic quadrupole moment $\langle Q_0^2 \rangle$ (in arbitrary units) and the quadrupole deformation parameter β_2 as a quantitative measure of the deformation. To understand the role of deformation on the NTME $M_{2\nu}$, we have investigated the variation of $\langle Q_0^2 \rangle$, β_2 and $M_{2\nu}$ with respect to the change in strength of the QQ interaction χ_{qq}. In table 4, we have presented the quadrupole moment of the intrinsic states $\langle Q_0^2 \rangle$, deformation parameter β_2 and the NTMEs $M_{2\nu}$ for different χ_{qq}. The deformation parameter has been calculated with the same effective charges as used in the calculation of $B(E2{:}\ 0^+ \to 2^+)$ transition probabilities. In general, $\langle Q_0^2 \rangle$ as well as β_2 increases as χ_{qq} is varied from 0 to 1.5 except a few anomalies. The intrinsic quadrupole moments show fluctuations in case of ^{96}Zr at χ_{qq} values 0.9 and 1.05. In case of ^{96}Mo and ^{100}Ru, similar fluctuations are observed at χ_{qq} equal to 0.2. In all the cases above discussed, it is found that the quadrupole deformation parameter β_2 follows the same behaviour as the quadrupole moment of the intrinsic state $\langle Q_0^2 \rangle$ with respect to the change in χ_{qq} except for the case of ^{94}Zr and ^{98}Ru. In case of ^{94}Zr, for a variation of χ_{qq} from 0.80 to 0.95, $\langle Q_0^2 \rangle$ increases but β_2 remains almost constant. For ^{98}Ru, β_2 decreases when χ_{qq} is varied from 0.2 to 0.4. Further, there is an anticorrelation between the deformation parameter and the NTME $M_{2\nu}$ in general.

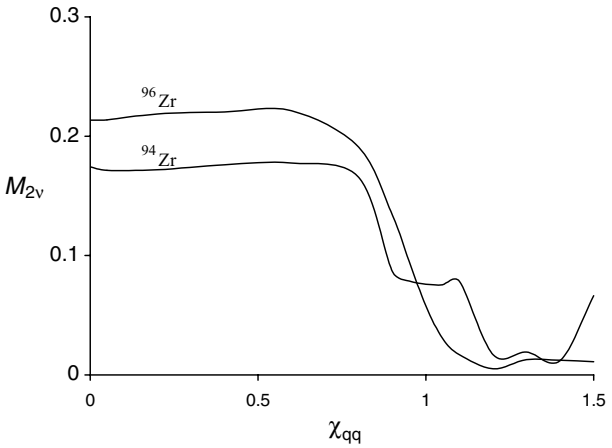

Fig. 1. The dependence of $M_{2\nu}$ of ^{94}Zr $\to$ ^{94}Mo and ^{96}Zr $\to$ ^{96}Mo on the strength of the QQ interaction χ_{qq} for the $0^+ \to 0^+$ transition.

In fig. 1, we have displayed the dependence of $M_{2\nu}$ on the χ_{qq} for the 2ν $\beta\beta$ decay of ^{94,96}Zr. In case of ^{94}Zr, $M_{2\nu}$ remains almost constant as the strength of χ_{qq} is changed from 0.00 to 0.80. As the strength of χ_{qq} is increased further up to 1.5, $M_{2\nu}$ decreases except at 1.1, 1.3 and 1.5, where there is an increase in the value of $M_{2\nu}$. In case of ^{96}Zr, $M_{2\nu}$ remains almost constant as χ_{qq} is changed from 0.00 to 0.60. $M_{2\nu}$ decreases as χ_{qq} is changed to 1.20. As χ_{qq} is further varied to 1.5, $M_{2\nu}$ increases initially and remains almost constant. In case of ^{96}Zr $\to$ ^{96}Mo, the experimental $M_{2\nu}$ is available. It is interesting to observe that $M_{2\nu}$ gets tuned towards the realistic value as χ_{qq} acquires a physical value around 1.0.

The dependence of $M_{2\nu}$ on χ_{qq} has been displayed for the 2ν $\beta\beta$ decay of ^{98,100}Mo in fig. 2. In case of ^{98}Mo, $M_{2\nu}$ remains almost constant as χ_{qq} is varied from 0.00 to 0.60 and then decreases, while χ_{qq} is changed to 1.2 except at 0.95. With further increase in χ_{qq}, $M_{2\nu}$ increases at $\chi_{qq} = 1.3$ and 1.4 and then decreases at $\chi_{qq} = 1.5$. In case of ^{100}Mo, $M_{2\nu}$ increases as χ_{qq} is varied from 0.00 to 0.80 and then decreases, while χ_{qq} is changed to 1.10 except at 0.95. There is a further increase in $M_{2\nu}$ as χ_{qq} is changed from 1.10 to 1.30 and then decreases up to 1.5. It is interesting to observe that in case of ^{100}Mo $\to$ ^{100}Ru,

Table 4. Effect of the variation in χ_{qq} on $\langle Q_0^2 \rangle$, β_2 and NTMEs $M_{2\nu}$.

	χ_{qq}	0.00	0.20	0.40	0.60	0.80	0.90	0.95	1.00	1.05	1.10	1.20	1.30	1.40	1.50
^{94}Zr	$\langle Q_0^2 \rangle$	0	0.021	0.065	0.121	0.308	3.698	4.275	18.47	22.68	26.12	31.76	37.90	40.62	50.90
	β_2	0	0.073	0.086	0.089	0.093	0.092	0.093	0.100	0.111	0.124	0.147	0.184	0.203	0.242
^{94}Mo	$\langle Q_0^2 \rangle$	0	0.011	0.041	1.488	14.39	26.40	28.64	31.15	33.78	36.37	59.11	60.76	61.62	62.54
	β_2	0	0.060	0.091	0.102	0.104	0.136	0.147	0.161	0.177	0.194	0.294	0.302	0.307	0.311
	$M_{2\nu}$	0.174	0.172	0.176	0.178	0.165	0.087	0.079	0.076	0.076	0.078	0.017	0.019	0.012	0.066
^{96}Zr	$\langle Q_0^2 \rangle$	0	0.050	0.116	0.485	1.254	0.368	0.463	2.484	1.919	2.540	5.446	34.20	39.02	40.70
	β_2	0	0.073	0.076	0.083	0.084	0.082	0.083	0.085	0.085	0.086	0.087	0.132	0.153	0.162
^{96}Mo	$\langle Q_0^2 \rangle$	0	0.696	0.211	0.477	22.46	31.82	37.02	41.73	45.15	48.15	61.43	65.44	66.70	67.64
	β_2	0	0.091	0.093	0.093	0.107	0.142	0.167	0.191	0.210	0.224	0.268	0.281	0.286	0.290
	$M_{2\nu}$	0.213	0.219	0.220	0.221	0.191	0.134	0.095	0.058	0.031	0.017	0.005	0.013	0.012	0.011
^{98}Mo	$\langle Q_0^2 \rangle$	0	0.222	0.620	0.894	1.681	6.531	35.14	42.33	46.33	48.70	51.24	53.51	64.59	71.42
	β_2	0	0.077	0.079	0.080	0.081	0.084	0.129	0.158	0.178	0.191	0.203	0.211	0.240	0.258
^{98}Ru	$\langle Q_0^2 \rangle$	0	0.084	0.091	14.52	37.14	43.80	47.08	51.73	72.45	75.10	77.66	79.27	82.80	86.52
	β_2	0	0.082	0.078	0.090	0.148	0.175	0.188	0.205	0.280	0.294	0.307	0.311	0.319	0.327
	$M_{2\nu}$	0.242	0.252	0.262	0.259	0.114	0.063	0.140	0.130	0.023	0.012	0.006	0.007	0.029	0.021
^{100}Mo	$\langle Q_0^2 \rangle$	0	0.034	0.126	0.357	1.040	3.624	41.85	49.20	53.40	55.14	57.89	60.15	64.55	77.90
	β_2	0	0.057	0.082	0.098	0.105	0.108	0.193	0.231	0.255	0.263	0.275	0.284	0.301	0.347
^{100}Ru	$\langle Q_0^2 \rangle$	0	0.193	0.116	1.131	2.707	38.30	42.95	45.66	48.04	49.81	52.92	57.60	81.92	83.00
	β_2	0	0.100	0.080	0.106	0.108	0.179	0.201	0.214	0.227	0.236	0.252	0.274	0.385	0.392
	$M_{2\nu}$	0.243	0.261	0.266	0.276	0.281	0.127	0.164	0.104	0.049	0.044	0.044	0.058	0.019	0.015
^{104}Ru	$\langle Q_0^2 \rangle$	0	0.043	0.154	0.506	44.77	56.58	60.55	63.98	67.60	71.04	76.11	90.61	92.32	92.70
	β_2	0	0.064	0.091	0.109	0.203	0.253	0.270	0.285	0.303	0.321	0.349	0.410	0.416	0.417
^{104}Pd	$\langle Q_0^2 \rangle$	0	0.015	0.055	0.223	0.698	37.42	44.53	48.85	52.03	54.91	59.66	65.01	90.55	91.26
	β_2	0	0.008	0.030	0.075	0.098	0.170	0.198	0.216	0.230	0.241	0.262	0.289	0.401	0.404
	$M_{2\nu}$	0.373	0.370	0.370	0.377	0.141	0.117	0.096	0.068	0.040	0.023	0.017	0.002	0.002	0.002
^{110}Pd	$\langle Q_0^2 \rangle$	0	0.061	0.136	0.398	34.79	47.92	53.10	57.39	60.67	63.70	71.74	79.01	83.03	84.47
	β_2	0	0.056	0.065	0.087	0.140	0.183	0.201	0.216	0.226	0.236	0.269	0.306	0.332	0.341
^{110}Cd	$\langle Q_0^2 \rangle$	0	0.028	0.073	0.191	11.54	37.99	44.88	54.59	69.99	77.13	80.21	81.99	83.77	85.77
	β_2	0	0.015	0.027	0.052	0.096	0.139	0.162	0.196	0.261	0.298	0.311	0.317	0.323	0.329
	$M_{2\nu}$	0.419	0.419	0.422	0.422	0.305	0.191	0.150	0.133	0.100	0.064	0.047	0.026	0.012	0.002

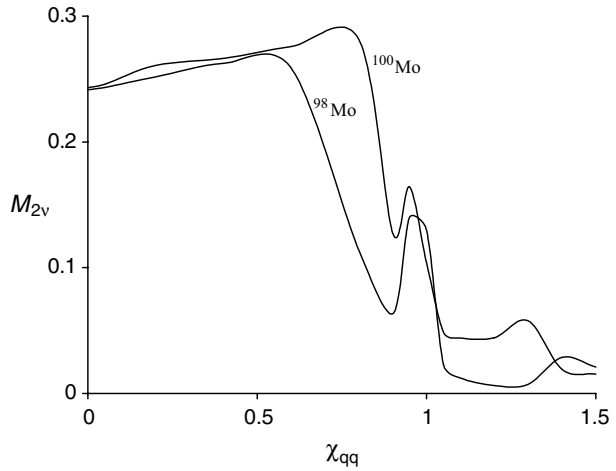

Fig. 2. The dependence of $M_{2\nu}$ of $^{98}\text{Mo} \rightarrow {}^{98}\text{Ru}$ and $^{100}\text{Mo} \rightarrow {}^{100}\text{Ru}$ on the strength of the QQ interaction χ_{qq} for the $0^+ \rightarrow 0^+$ transition.

$M_{2\nu}$ also gets tuned towards the realistic value as χ_{qq} acquires a physical value around 1.0.

In fig. 3, we have displayed the dependence of $M_{2\nu}$ on χ_{qq} for the 2ν $\beta\beta$ decay of ^{104}Ru and ^{110}Pd. $M_{2\nu}$ remains almost constant as χ_{qq} is varied from 0.00 to 0.60 and then decreases as χ_{qq} is changed from 0.6 to 1.5 in case of ^{104}Ru and ^{110}Pd. To summarize, we have shown that the deformations of the HFB intrinsic states play an important role in reproducing a realistic $M_{2\nu}$.

To quantify the effect of deformation on $M_{2\nu}$, we define a quantity $D_{2\nu}$ as the ratio of $M_{2\nu}$ at zero deformation ($\chi_{qq} = 0$) and full deformation ($\chi_{qq} = 1$). $D_{2\nu}$ is given by

$$D_{2\nu} = \frac{M_{2\nu}(\chi_{qq} = 0)}{M_{2\nu}(\chi_{qq} = 1)} \,. \tag{21}$$

The values of $D_{2\nu}$ are 2.29, 3.70, 1.86, 2.33, 5.47 and 3.14 for ^{94,96}Zr,^{98,100}Mo,^{104}Ru and ^{110}Pd nuclei, respectively. These values of $D_{2\nu}$ suggest that $M_{2\nu}$ is quenched by a factor of approximately 2 to 5.5 in the mass region $94 \leq A \leq 110$ due to deformation effects.

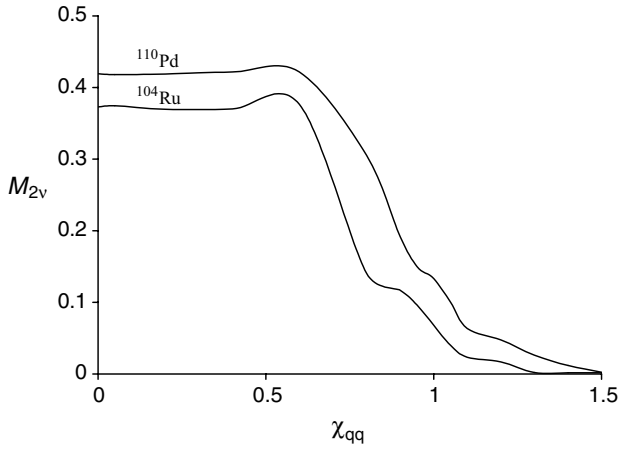

Fig. 3. The dependence of $M_{2\nu}$ of $^{104}\mathrm{Ru} \to {}^{104}\mathrm{Pd}$ and $^{110}\mathrm{Ru} \to {}^{110}\mathrm{Pd}$ on the strength of the QQ interaction χ_{qq} for the $0^+ \to 0^+$ transition.

4 Conclusions

As a first step, we have tested the quality of HFB wave functions by comparing the theoretically calculated results for a number of spectroscopic properties of ^{94,96}Zr, ^{94,96,98,100}Mo, ^{98,100,104}Ru, ^{104,110}Pd and ^{110}Cd nuclei with the available experimental data. To be more specific, we have computed the yrast spectra, reduced $B(E2: 0^+ \to 2^+)$ transition probabilities, quadrupole moments $Q(2^+)$ and g-factors $g(2^+)$. Subsequently, the reliability of the intrinsic wave functions has been tested by calculating $M_{2\nu}$ of ^{96}Zr and ^{100}Mo, for which the 2ν $\beta\beta$ decay has already been measured. In case of ^{96}Zr and ^{100}Mo, the agreement between the theoretically calculated and experimentally observed $M_{2\nu}$ as well as $T^{2\nu}_{1/2}$ makes us confident to predict the half-lives $T^{2\nu}_{1/2}$ for other nuclei undergoing the 2ν $\beta\beta$ decay in the mass region $94 \leq A \leq 110$. For ^{94}Zr,^{98}Mo,^{104}Ru and ^{110}Pd isotopes, the values of $T^{2\nu}_{1/2}$ for $g_A = 1.25$–1.00 are $(7.51$–$18.34) \times 10^{22}$ y, $(6.09$–$14.87) \times 10^{29}$ y, $(2.35$–$5.73) \times 10^{22}$ y and $(1.41$–$3.44) \times 10^{20}$ y, respectively.

Further, we have shown that the deformations of the intrinsic ground states of ^{96}Zr, ^{96,100}Mo and ^{100}Ru play a crucial role in reproducing a realistic NTME in case of ^{96}Zr and ^{100}Mo. The NTMEs $M_{2\nu}$ are quenched by a factor of approximately 2 to 5.5 in the mass region $94 \leq A \leq 110$ due to the deformation. A reasonable agreement between the calculated and observed spectroscopic properties of ^{94,96}Zr, ^{94,96,98,100}Mo, ^{98,100,104}Ru, ^{104,110}Pd and ^{110}Cd as well as the 2ν $\beta\beta$ decay rate of ^{94,96}Zr,^{98,100}Mo,^{104}Ru and ^{110}Pd makes us confident to employ the same PHFB wave functions to study the 0ν $\beta\beta$ decay, which will be communicated in the future.

P.K. Rath would like to acknowledge the financial support provided by CTS, IIT, Kharagpur, where the present work has been finalized. Further, R. Chandra is grateful to CSIR, India for providing Senior research fellowship *vide* award No. 9/107(222)/2KI/EMR-I.

References

1. M. Goeppert-Mayer, Phys. Rev. **48**, 512 (1935).
2. W. Fury, Phys. Rev. **56**, 1184 (1939).
3. D. Bryman, C. Picciotto, Rev. Mod. Phys. **50**, 11 (1978).
4. H. Primakoff, S.P. Rosen, Annu. Rev. Nucl. Part. Sci. **31**, 145 (1981).
5. W.C. Haxton, G.J. Stephenson jr., Prog. Part. Nucl. Phys. **12**, 409 (1984).
6. M. Doi, T. Kotani, E. Takasugi, Prog. Theor. Phys. Suppl. **83**, 1 (1985).
7. J.D. Vergados, Phys. Rep. **133**, 1 (1986); **361**, 1 (2002).
8. A. Faessler, Prog. Part. Nucl. Phys. **21**, 183 (1988).
9. T. Tomoda, Rep. Prog. Phys. **54**, 53 (1991).
10. F. Boehm, P. Vogel, Annu. Rev. Nucl. Part. Sci. **34**, 125 (1984); *Physics of Massive Neutrinos*, 2nd edition (Cambridge University Press, Cambridge, 1992).
11. M.K. Moe, P. Vogel, Annu. Rev. Nucl. Part. Sci. **44**, 247 (1994).
12. J. Suhonen, O. Civitarese, Phys. Rep. **300**, 123 (1998).
13. A. Faessler, F. Simkovic, J. Phys. G **24,** 2139 (1998), hep-ph/9901215.
14. H.V. Klapdor (Editor), *Proceedings of the International Symposium on Weak and Electromagnetic Interactions in Nuclei* (Springer, Berlin, 1986); *Neutrinos* (Springer, Heidelberg, 1988); H.V. Klapdor, S. Stoica (Editors), *Proceedings of the International Workshop on Double Beta Decay and Related Topics, Trento, Italy, 1995* (World Scientific, Singapore, 1996); H.V. Klapdor-Kleingrothaus, hep-ex/9907040, hep-ex/9901021, hep-ex/9802007; Int. J. Mod. Phys. A **13**, 3953 (1998).
15. K. Zuber, Phys. Rep. **305**, 295 (1998).
16. E. Fiorini, Phys. Rep. **307**, 309 (1998).
17. H. Ejiri, Phys. Rep. **338**, 265 (2000).
18. S.R. Elliott, P. Vogel, hep-ph./0202264.
19. V.I. Tretyak, Y.G. Zdesenko, At. Data Nucl. Data Tables **61**, 43 (1995); **80**, 83 (2002).
20. H.V. Klapdor-Kleingrothaus, A. Dietz, H.L. Harney, I.V. Krivosheina, hep-ph/0201231; C.E. Aalseth *et al.*, hep-ex/0202018; Yu. G. Zdesenko, F.A. Danevich, V.I. Tretyak, Phys. Lett. B **546**, 206 (2002).
21. L. Zhao, B.A. Brown, W.A. Richter, Phys. Rev. C **42**, 1120 (1990); H. Nakada, T. Sebe, K. Muto, Nucl. Phys. A **607**, 235 (1996); J. Suhonen, P.C. Divari, L.D. Skouras, I.P. Johnstone, Phys. Rev. C **55**, 714 (1997).
22. E. Caurier, F. Nowacki, A. Poves, J. Retamosa, Phys. Rev. Lett. **77**, 1954 (1996).
23. P.B. Radha, D.J. Dean, S.E. Koonin, T.T.S. Kuo, K. Langanke, A. Poves, J. Retamosa, P. Vogel, Phys. Rev. Lett. **76**, 2642 (1996); S.E. Koonin, D.J. Dean, K. Langanke, Phys. Rep. **278**, 1 (1997).
24. P. Vogel, M.R. Zirnbauer, Phys. Rev. Lett. **57**, 3148 (1986).
25. B.M. Dixit, P.K. Rath, P.K. Raina, Phys. Rev. C **65**, 034311 (2002); **67**, 059901(E) (2003).
26. K. Chaturvedi, B.M. Dixit, P.K. Rath, P.K. Raina, Phys. Rev. C **67**, 064317 (2003).
27. O. Civitarese, J. Suhonen, Phys. Rev. C **47**, 2410 (1993).
28. E. Cheifetz *et al.*, Phys. Rev. Lett. **25**, 38 (1970).
29. A. Griffiths, P. Vogel, Phys. Rev. C **46**, 181 (1992).
30. J. Suhonen, O. Civitarese, Phys. Rev. C **49**, 3055 (1994).

31. S.K. Khosa, P.N. Tripathi, S.K. Sharma, Phys. Lett. B **119**, 257 (1982); P.N. Tripathi, S.K. Sharma, S.K. Khosa, Phys. Rev. C **29**, 1951 (1984); S.K. Sharma, P.N. Tripathi, S.K. Khosa, Phys. Rev. C **38**, 2935 (1988).
32. M. Baranger, K. Kumar, Nucl. Phys. A **110**, 490 (1968).
33. O. Castaños, J.G. Hirsch, O. Civitarese, P.O. Hess, Nucl. Phys. A **571**, 276 (1994).
34. J.G. Hirsch, O. Castaños, P.O. Hess, O. Civitarese, Phys. Rev. C **51**, 2252 (1995).
35. V.E. Ceron, J.G. Hirsch, Phys. Lett. B **471**, 1 (1999).
36. J.D. Vergados, T.T.S. Kuo, Phys. Lett. B **35**, 93 (1971); P. Federman, S. Pittel, Phys. Lett. B **77**, 29 (1978).
37. G.M. Heestand, R.R. Borchers, B. Herskind, L. Grodzins, R. Kalish, D.E. Murnick, Nucl. Phys. A **133**, 310 (1969).
38. W. Greiner, Nucl. Phys. **80**, 417 (1966).
39. A. Arima, Nucl. Phys. A **354**, 19 (1981).
40. M. Sakai, At. Data Nucl. Data Tables **31**, 400 (1984).
41. S. Raman, C.W. Nestor jr., S. Kahane, K.H. Bhatt, At. Data Nucl. Data Tables, **36**, 1 (1987).
42. P. Raghavan, At. Data Nucl. Data Tables **42**, 189 (1989); A. Giannatiempo, A. Nannini, P. Sona, D. Cutoiu, Phys. Rev. C **52**, 2969 (1995); A. Bockisch, A.M. Kleinfeld, Nucl. Phys. A **261**, 498 (1976)
43. K.H. Speidel, O. Kenn, F. Nowacki, Prog. Part. Nucl. Phys. **49**, 91 (2002).
44. R. Arnold *et al.*, Nucl. Phys. A **658**, 299 (1999).
45. A. Staudt, K. Muto, H.V. Klapdor, Europhys. Lett. **13**, 31 (1990).
46. M. Hirsch, X.R. Wu, H.V. Klapdor-Kleingrothaus, Ching Cheng-rui, Ho Tso-hsiu, Phys. Rep. **242**, 403 (1994).
47. A. Bobyk, W.A. Kaminski, P. Zareba, Nucl. Phys. A **669**, 221 (2000).
48. A. Kawashima, K. Takahashi, A. Masuda, Phys. Rev. C **47**, 2452 (1993).
49. A.S. Barabash, Nucl. Phys. A **629**, 517c (1998).
50. M.E. Wieser, John R. De Laeter, Phys. Rev. C **64**, 024308 (2001).
51. A.S. Barabash, Czech. J. Phys. **52**, 567 (2002).
52. J. Engel, P. Vogel, M.R. Zirnbauer, Phys. Rev. C **37**, 731 (1988).
53. S. Stoica, Phys. Lett. B **350**, 152 (1995).
54. A.S. Barabash, R. Gurriaran, F. Hubert, Ph. Hubert, J.L. Reyss, J. Suhonen, V.I. Umatov, J. Phys. G **22**, 487 (1996).
55. J. Toivanen, J. Suhonen, Phys. Rev. C **55**, 2314 (1997).
56. O.A. Rumyantsev, M.H. Urin, Phys. Lett. B **443**, 51 (1998).
57. S.I. Vasilev *et al.*, JETP Lett. **51**, 622 (1990); **58**, 178 (1993).
58. S.R. Elliott, M.K. Moe, M.A. Nelson, M.A. Vient, J. Phys. G **17**, S145 (1991).
59. H. Ejiri *et al.*, J. Phys. G **17**, 155 (1991).
60. A. Garcia *et al.*, Phys. Rev. C **47**, 2910 (1993).
61. NEMO Collaboration (D. Dassie *et al.*), Phys. Rev. D **51**, 2090 (1995).
62. M. Alston Garnjost *et al.*, Phys. Rev. C **55**, 474 (1997).
63. A. De Silva, M.K. Moe, M.A. Nelson, M.A. Vient, Phys. Rev. C **56**, 2451 (1997).
64. V.D. Ashitkov *et al.*, Phys. At. Nucl. **62**, 2044 (1999).
65. V.D. Ashitkov *et al.*, JETP Lett. **74**, 529 (2001).
66. J.G. Hirsch, O. Castaños, P.O. Hess, O. Civitarese, Phys. Rev. C **51**, 2252 (1995).
67. O. Civitarese, J. Suhonen, Phys. Rev. C **58**, 1535 (1998).
68. F. Simkovic, P. Domin, S.V. Semenov, nucl-th/0006084.
69. R.G. Winter, Phys. Rev. **85**, 687 (1952).
70. S. Stoica, Phys. Rev. C **49**, 2240 (1994).
71. S.V. Semenov, F. Simcovic, V.V. Khruschev, P. Domin, Phys. At. Nucl. **63**, 1196 (2000).